Studies of the Kinetics and Thermochemistry of the Forward and Reverse Reaction Cl + C_6H_6 = HCl + C_6H_5†

I. M. Alecu,‡ Yide Gao,‡ P-C. Hsieh,‡ Jordan P. Sand,§ Ahmet Ors,‡ A. McLeod,‡ and Paul Marshall*,‡

Department of Chemistry, University of North Texas, P.O. Box 305070, Denton, Texas 76203-5070, and Whitworth College, 300 West Hawthorne Road, Spokane, Washington 99251

Received: November 1, 2006; In Final Form: December 31, 2006

The laser flash photolysis resonance fluorescence technique was used to monitor atomic Cl kinetics. Loss of Cl following photolysis of CCl_4 and NaCl was used to determine $k(Cl + C_6H_6) = 6.4 \times 10^{-12}$ exp(−18.1 kJ mol^{-1}/*RT*) cm^3 molecule^{-1} s^{-1} over 578−922 K and $k(Cl + C_6D_6) = 6.2 \times 10^{-12}$ exp(−22.8 kJ mol^{-1}/*RT*) cm^3 molecule^{-1} s^{-1} over 635−922 K. Inclusion of literature data at room temperature leads to a recommendation of $k(Cl + C_6H_6) = 6.1 \times 10^{-11}$ exp(−31.6 kJ mol^{-1}/*RT*) cm^3 molecule^{-1} s^{-1} for 296−922 K. Monitoring growth of Cl during the reaction of phenyl with HCl led to $k(C_6H_5 + HCl) = 1.14 \times 10^{-12}$ exp(+5.2 kJ mol^{-1}/*RT*) cm^3 molecule^{-1} s^{-1} over 294−748 K, $k(C_6H_5 + DCl) = 7.7 \times 10^{-13}$ exp(+4.9 kJ mol^{-1}/*RT*) cm^3 molecule^{-1} s^{-1} over 292−546 K, an approximate $k(C_6H_5 + C_6H_5I) = 2 \times 10^{-11}$ cm^3 molecule^{-1} s^{-1} over 300−750 K, and an upper limit $k(Cl + C_6H_5I) \leq 5.3 \times 10^{-12}$ exp(+2.8 kJ mol^{-1}/*RT*) cm^3 molecule^{-1} s^{-1} over 300−750 K. Confidence limits are discussed in the text. Third-law analysis of the equilibrium constant yields the bond dissociation enthalpy $D_{298}(C_6H_5-H) = 472.1 \pm 2.5$ kJ mol^{-1} and thus the enthalpy of formation $\Delta_f H_{298}(C_6H_5) = 337.0 \pm 2.5$ kJ mol^{-1}.

1. Introduction

The phenyl radical is important in combustion chemistry because it is an intermediate in soot formation.[1] There have been several kinetic measurements on the reaction

$$Cl + C_6H_6 \rightarrow HCl + C_6H_5 \qquad (1)$$

at room temperature, made with relative rate techniques. The motivation was to gain insight into the atmospheric chemistry of aromatic species and to explore the utility of eq 1 in smog chamber experiments. Equation 1 may also be significant in the incineration of chlorine containing waste. The first measurements, by Atkinson and Aschmann,[2] indicated rapid reaction with a rate constant $k_1 = (1.5 \pm 0.9) \times 10^{-11}$ cm^3 molecule^{-1} s^{-1}. However, two subsequent studies yielded lower reactivities, with the work of Wallington et al.[3] and Nozière et al.[4] yielding upper limits to k_1 of $\leq 4 \times 10^{-12}$ and $\leq 5 \times 10^{-16}$ cm^3 molecule^{-1} s^{-1}, respectively. Shi and Bernhard obtained a contradictory value of $(1.3 \pm 0.3) \times 10^{-15}$ cm^3 molecule^{-1} s^{-1}.[5] The latter result is in disagreement with the most recent value of $(1.3 \pm 1.0) \times 10^{-16}$ cm^3 molecule^{-1} s^{-1} found by Sokolov et al.[6] These differences have not been resolved, although attention has been drawn to the possibilities of secondary chemistry and interference by impurities, which may complicate the relative rate experiments.[5,6] By a combination of time-resolved and relative rate measurements, Sokolov et al.[6] showed that the reactants rapidly formed a small concentration of a weakly bound adduct, which at room temperature slowly yielded HCl. Here, we present absolute rate results derived via the flash photolysis resonance fluorescence technique and the first investigation of the temperature dependence of k_1.

We have also made the first determination of the rate constant k_{-1} for the reverse process

$$C_6H_5 + HCl \rightarrow Cl + C_6H_6 \qquad (-1)$$

which in combination with k_1 data yields the equilibrium constant K_{eq}, through which thermodynamic information about the phenyl radical may be obtained. These results check recent revisions to the C_6H_5-H bond dissociation enthalpy D_{298}, which are based on the ion chemistry of Davico et al.[7] and the interpretation of several kinetic experiments by Heckmann et al.[8] A negative activation energy E_a is found for eq −1. Negative E_a values have been observed earlier in the case of alkyl and silyl radical reactions with HBr and HI,[9−14] although these experiments have been criticized.[15] The present results extend the scope of the phenomenon to aryl radical plus HCl chemistry.

The primary kinetic isotope effects in the two reactions, for which there are no prior data, are investigated via the equations

$$Cl + C_6D_6 \rightarrow DCl + C_6D_5 \qquad (1b)$$

and

$$C_6H_5 + DCl \rightarrow Cl + C_6H_5D \qquad (-1c)$$

The present work also provides some kinetic information about the reactions of phenyl iodide with Cl and C_6H_5. The former process has been studied once at room temperature,[16] while there appears to be no literature information for the latter.

† Part of the special issue "James A. Miller Festschrift".

* To whom correspondence should be addressed. E-mail: marshall@unt.edu.

‡ University of North Texas.

§ Whitworth College.

10.1021/jp067212o CCC: $37.00 © 2007 American Chemical Society
Published on Web 02/07/2007

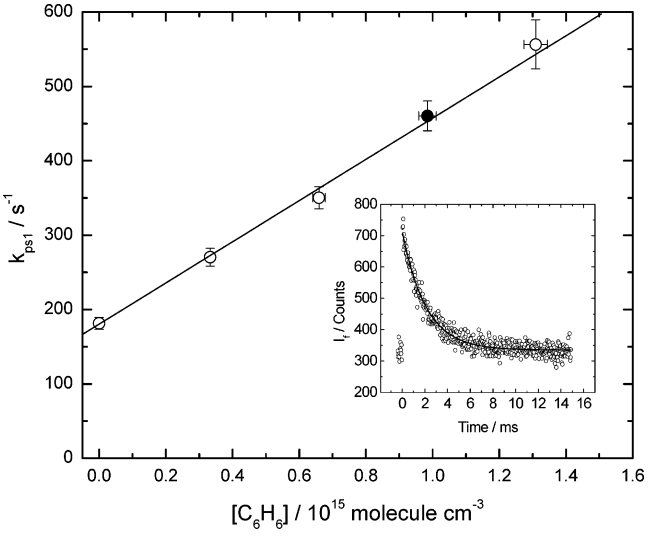

Figure 1. Pseudo-first-order decay coefficient for Cl in the presence of excess C_6H_6 at 676 K and 69 mbar total pressure with Ar. Error bars represent $\pm 1\sigma$. The inset shows the signal corresponding to the filled point.

2. Methodology

2.1. Measurements of Cl + C_6H_6 → HCl + C_6H_5. Argon (purity 99.9997%, Air Liquide) was used as supplied as the bath gas. Benzene (purity ≥99.9%) and benzene-d6 (atom purity 99.6%) were obtained from Aldrich, and tetrachloromethane (purity ≥99.9%) was obtained from Spectrum. The organic materials were separated from more volatile species via freeze−pump−thaw cycles at 77 K. We applied the flash-photolysis resonance fluorescence approach as detailed in previous studies.[17,18] Briefly, in the temperature range 578−724 K, atomic Cl was generated from the pulsed photolysis of CCl_4 at 193 nm using an excimer laser (MPB PSX-100, beam cross section 7×8 mm^2). The initial Cl concentration, $[Cl]_0$, was estimated using the measured laser output energy F, the beam cross section, and the CCl_4 absorption cross section which is $(8.6 \pm 0.5) \times 10^{-19}$ cm^2 (base e) at room temperature.[19] We neglected any variation of this cross section with temperature and used a quantum yield for Cl formation of 1.5.[19] This calculation does not account for the strong absorption of 193-nm radiation by benzene and therefore yields an upper limit to $[Cl]_0$. $[Cl]_0$ does not need to be known for the kinetic analysis, but an approximate assessment of its concentration is convenient for assurance that $[Cl] \ll [C_6H_6]$. As noted by Adusei and Fontijn,[20] at higher temperatures CCl_4 is unsatisfactory, and accordingly at 922 K we employed their suggestion of NaCl(g) as the photolytic precursor for Cl. NaCl evaporated from a porcelain boat in the gas entry sidearm. The partial pressure of NaCl is not known under these conditions and therefore nor is $[Cl]_0$ with this photolyte. The Cl atoms were monitored by time-resolved resonance fluorescence at 130−140 nm with photon counting and signal averaging, were excited with a microwave flow lamp, and were observed through calcium fluoride optics. Argon bath gas maintains thermal equilibrium and slows diffusion of atomic Cl to the reactor walls. Exponential decays of the fluorescence signal I_f were observed, as seen in the inset of Figure 1. We interpret these via the relation

$$d[Cl]/dt = -k_1[Cl][C_6H_6] - k'[Cl] = -k_{ps1}[Cl]$$

where k' accounts for diffusional loss of Cl and consumption by secondary processes such as reaction with photolysis or reaction products. A large excess of benzene imposed pseudo-first-order kinetics, and the resulting exponential decay coefficients k_{ps1} were derived by fitting the concentration of Cl as a function of time t to the integrated rate law

$$[Cl] = [Cl]_0 \exp(-k_{ps1}t)$$

Figure 1 is an example of a plot of k_{ps1} against $[C_6H_6]$. Statistical errors in k_{ps1} were obtained from the fitting algorithm.[21,22] Typically, five values were employed at a given set of conditions, from zero to $[C_6H_6]_{max}$. Linear least-squares analysis, with weighting for errors in concentration and in k_{ps1},[23] yielded the slope, which is equal to the second-order rate constant k_1 and the intercept k'. The statistical uncertainty in the slope was combined in quadrature with the estimated reproducibility of the gas flows, pressure, and temperature T, 2.5%. The average value of the intercept was found to lie in the range 50−100 s^{-1} below 650 K but increased to over 250 s^{-1} at the higher temperatures. Experimental parameters such as the photolysis energy F, the photolyte concentration, the total pressure, and the average gas residence time inside the reactor, τ_{res}, were varied to assess any dependence of the observed rate constants k_1 upon such parameters. k_{1b} was obtained with C_6D_6 instead of benzene.

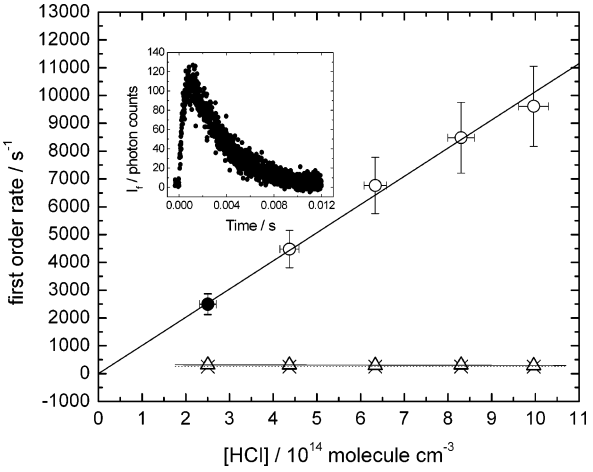

Figure 2. First-order rates in fit to Cl growth and decay in the C_6H_5 + HCl reaction at 294 K and 65 total pressure with Ar. Circles: k_1-[HCl]; open triangles: $k_2[C_6H_5] + k_3$; crosses: $k_4[C_6H_5]$. Error bars represent $\pm 1\sigma$. The inset shows a signal corresponding to the filled circle.

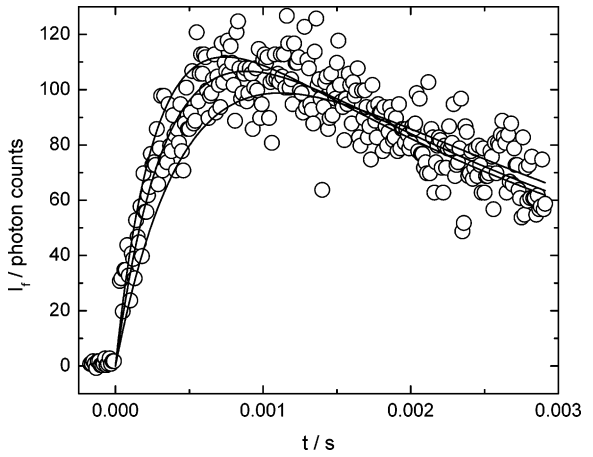

Figure 3. Example of fit to Cl growth and decay signal (background subtracted) at 294 K. The central line is the best fit, and the upper and lower lines represent the effect of increasing or reducing the B parameter by 30%, taken to approximate $\pm 2\sigma$.

TABLE 1: Summary of Measurements of the Rate Constant k_1 for Cl + C_6H_6

T, K	τ_{res}, s	F, mJ	p, mbar	$[CCl_4]$, 10^{15} molecule cm^{-3}	$[C_6H_6]_{max}$, 10^{15} molecule cm^{-3}	$[Cl]_0$, 10^{12} molecule cm^{-3}	$k_1 \pm \sigma_{k1}$, 10^{-13} cm^3 molecule^{-1} s^{-1}
579	1.0	0.26	70	2.40	5.31 ± 0.18	0.9	2.16 ± 0.06
578	1.0	0.24	71	1.48	1.36 ± 0.05	0.5	2.20 ± 0.18
578	1.0	0.16	71	1.48	1.36 ± 0.06	0.3	1.91 ± 0.11
577	1.1	0.21	145	1.63	1.12 ± 0.02	0.5	2.02 ± 0.10
578[a]							**1.49 ± 0.10**[b]
622	0.9	0.44	67	2.00	1.87 ± 0.06	1.4	3.26 ± 0.25
622	0.9	0.19	67	2.00	1.87 ± 0.06	0.6	2.70 ± 0.10
621	0.9	0.19	69	2.05	1.92 ± 0.07	0.6	2.13 ± 0.07
621	0.9	0.06	69	2.05	1.92 ± 0.07	0.2	1.90 ± 0.08
619	0.5	0.09	71	1.21	1.64 ± 0.05	0.2	1.60 ± 0.08
623	0.9	0.35	70	2.02	2.96 ± 0.10	1.0	1.99 ± 0.12
623	0.9	0.16	70	2.02	2.96 ± 0.06	0.5	1.70 ± 0.06
622	2.0	0.33	145	2.62	3.25 ± 0.11	1.2	2.00 ± 0.31
622	2.0	0.13	145	2.62	3.25 ± 0.07	0.5	1.78 ± 0.32
622[a]							**1.60 ± 0.26**[b]
676	0.4	0.33	29	0.88	1.66 ± 0.06	0.5	2.61 ± 0.18
676	0.4	0.14	29	0.88	1.66 ± 0.06	0.2	2.35 ± 0.15
677	0.9	0.21	70	1.23	2.69 ± 0.09	0.5	2.79 ± 0.36
677	0.9	0.14	70	1.23	2.69 ± 0.07	0.3	2.75 ± 0.23
674	0.5	0.17	69	1.21	1.31 ± 0.03	0.3	2.71 ± 0.07
674	0.5	0.11	69	1.21	1.31 ± 0.03	0.2	2.77 ± 0.09
676[a]							**2.76 ± 0.19**[b]
725	1.2	0.53	76	2.59	1.96 ± 0.09	2.0	5.66 ± 0.32
725	0.9	0.74	77	1.94	2.03 ± 0.07	2.1	6.07 ± 0.21
725	0.9	0.50	77	1.94	2.03 ± 0.07	1.4	5.10 ± 0.23
725	0.9	0.34	77	1.94	2.03 ± 0.07	0.9	4.60 ± 0.10
722	1.0	0.34	152	1.41	2.33 ± 0.06	0.8	4.09 ± 0.23
722	1.0	0.23	152	1.41	2.33 ± 0.06	0.5	3.83 ± 0.16
722	1.0	0.15	152	1.41	2.33 ± 0.06	0.3	3.80 ± 0.10
724[a]							**3.14 ± 0.16**[b]
922	0.4	0.99	41	[d]	0.57 ± 0.02		7.84 ± 0.57
922	0.4	0.46	41	[d]	0.57 ± 0.02		5.75 ± 0.59
922	0.4	0.60	41	[d]	0.94 ± 0.05		2.70 ± 0.55
922	0.4	0.28	41	[d]	0.94 ± 0.05		2.58 ± 0.56
921	0.4	0.83	43	[d]	0.48 ± 0.02		6.77 ± 1.65
921	0.4	0.38	43	[d]	0.48 ± 0.02		4.73 ± 0.40
922[a]							**5.06 ± 2.14**[c]

[a] Average temperature. [b] Extrapolation to zero F. [c] Mean value. [d] NaCl used as Cl source rather than CCl_4.

2.2. Measurements of C_6H_5 + HCl → Cl + C_6H_6. Phenyl iodide (purity 98%) and hydrogen chloride gas (purity ≥99.9%) from Aldrich were purified via freeze−pump−thaw cycles at 77 K. Phenyl radicals were generated by 193-nm photolysis of C_6H_5I, and the initial concentration $[C_6H_5]_0$ was estimated similarly to $[Cl]_0$ in the previous section, on the basis of the room-temperature C_6H_5I absorption cross section of approximately 6.5×10^{-17} cm^2 molecule^{-1} (base e).[24] We assumed a quantum yield of 1 and therefore obtained an upper limit to $[C_6H_5]_0$. Phenyl was allowed to react with excess HCl in an Ar bath gas, and the atomic Cl product of eq −1 was monitored as outlined above. The following mechanism was used to interpret the Cl fluorescence signals:

$$C_6H_5 + HCl \xrightarrow{k_{-1}} Cl + C_6H_6 \qquad (-1)$$

$$C_6H_5I + Cl \xrightarrow{k_2} \text{products} \qquad (2)$$

$$Cl \xrightarrow{k_3} \text{diffusion} \qquad (3)$$

$$C_6H_5 + C_6H_5I \xrightarrow{k_4} \text{products} \qquad (4)$$

Cl is formed by eq −1 and is lost by diffusion and potentially via reaction 2 with C_6H_5I. Equation 4 competes with eq 1 to consume phenyl radicals. The corresponding integrated rate law is

$$\frac{AB}{(B+D)-C}(e^{-Ct} - e^{-(B+D)t})$$

where

$$A = [C_6H_5]_0 \quad B = k_{-1}[HCl] \quad C = k_2[C_6H_5I] + k_3 \quad D = k_4[C_6H_5I]$$

An example fluorescence signal is shown as the inset in Figure 2. After subtraction of a constant background arising from scattered resonance radiation, as determined from the pretrigger signal, the signal was fit by varying the $A-D$ parameters. Cl profiles were obtained as a function of typically five values of [HCl], and Figure 2 shows a plot of the B parameter versus [HCl]. The slope yields the reverse rate constant k_{-1}, and the intercept is close to zero as expected. The uncertainty in B was estimated by seeing how much variation in this parameter could be tolerated in fits to the Cl signal. An example is shown in Figure 3 , which shows the effect of changing B by ±30%, which is taken as an estimate of 2σ for B. As may also be seen in Figure 2, C and D are essentially constant and small compared to B, so that errors in these terms have little impact on k_{-1}. The above mechanism is based on the assumption that no other photolytically produced species generate atomic Cl. A potential

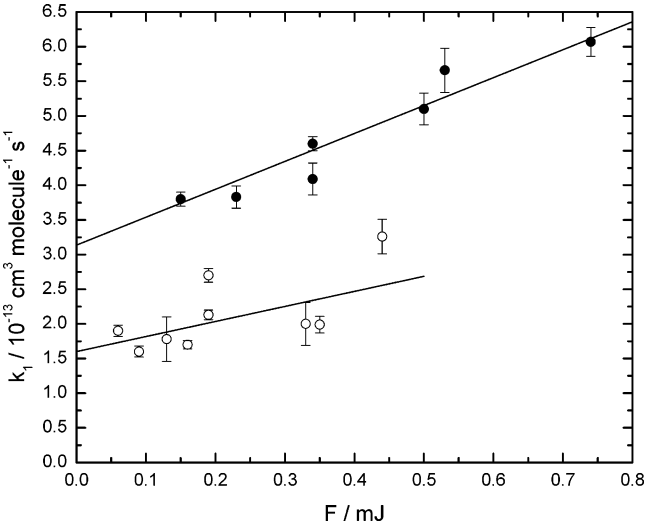

Figure 4. Dependence of observed k_1 on laser photolysis energy F at 622 K (open circles) and 724 K (solid circles). Error bars represent $\pm 1\sigma$.

interference is atomic H, which could react with HCl to make H_2 + Cl. Not only is this reaction too slow to interfere except at the highest temperature we studied,[25] but also the yield of H from 193-nm photolysis of C_6H_5I appears to be small. We photolyzed phenyl iodide while monitoring H-atoms by resonance fluorescence at 121 nm and observed no H signal. By comparison with experiments where phenyl iodide was photolyzed in the presence of excess H_2 (which converts C_6H_5 to C_6H_6 + H), we deduce an upper limit of H-atom production to be 5% of phenyl production. Absorption of 193-nm photons could populate a variety of electronic states of C_6H_5I whose fate is unknown, although we speculate they may be removed rapidly by collisional quenching, emission, or internal conversion.

The concentration of photolyte, [C_6H_5I], was not varied systematically but an approximate estimate of k_4 is obtained by dividing the D parameter by [C_6H_5I]. Similarly, division of the C parameter by [C_6H_5I] yields an estimated k_2. Strictly, this is an upper limit because of the neglect of the unknown diffusional contribution k_3. The k' term in the CCl_4 photolysis experiments may be similar to k_3, but k' also includes contributions from secondary chemistry which is likely to be different in the C_6H_5I/HCl system. HCl mixtures were flowed through the reactor at least an hour before experiments were begun to passivate surfaces in the apparatus. The observed constancy of the kinetics over ~5 h confirms that HCl was not lost significantly on the reactor walls during the measurements.

In some experiments, DCl was used instead of HCl. Deuterium chloride was synthesized by exposing a mixture of about 30 mbar Cl_2 with about 60 mbar D_2 in a 20-L Pyrex bulb to UV radiation from a mercury pen-ray lamp for 2 days. The use of low pressures avoids an explosion. DCl was separated from the reaction mixture by freeze−pump−thaw cycles and distillation from an acetone slush at 178 K.

Results

3.1. Rate Constants. Table 1 summarizes 32 determinations of k_1. At the low end of the temperature range, we observe a dependence of the observed k_1 value on the photolysis pulse energy F. Examples are shown in Figure 4. The dependence was extrapolated to zero F via a weighted linear least-squares fit to obtain k_1 in the absence of secondary chemistry, and these values are also listed in Table 1 along with the statistical

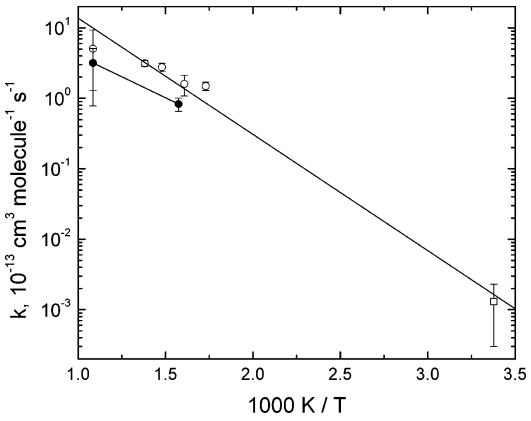

Figure 5. Arrhenius plot of k_1 and k_{1b}. Open circles and square: Cl + C_6H_6, this work and Sokolov et al.;[6] filled circles: Cl + C_6D_6, this work. Error bars represent $\pm 2\sigma$.

uncertainty in these intercepts. This phenomenon set the lower temperature bound to our measurements, because as the intercept becomes small the percentage uncertainty becomes large. At the highest temperature, no systematic variation with F was found, and instead the measurements were averaged. Variation of other parameters such as pressure and residence time had no consistent influence, which indicates that mixing or thermal decomposition had no large effect.

Figure 5 shows an Arrhenius plot of the k_1 data, which may be represented as

$$k_1 = (6.4 \pm 2.8) \times 10^{-12} \exp(-18.1 \pm 2.3 \text{ kJ mol}^{-1}/RT) \text{ cm}^3 \text{ molecule}^{-1} \text{ s}^{-1}$$

over 578−922 K. This fit incorporates statistical uncertainty in k_1 and in temperature ($\sigma_T/T = 2\%$). One σ uncertainties in the Arrhenius parameters are shown above, and together with the covariance they yield 2σ statistical uncertainties in the fitted k_1 of between 6 and 24%. Allowance for potential systematic errors of around 10% yields overall 95% confidence limits of ±26%. The range of k_1 data can be extended down to 296 K by incorporating the measurement of Sokolov et al.[6] An unweighted fit to the combined data set yields the recommendation

$$k_1 = (6.1 \pm 3.2) \times 10^{-11} \exp(-31.6 \pm 2.1 \text{ kJ mol}^{-1}/RT) \text{ cm}^3 \text{ molecule}^{-1} \text{ s}^{-1}$$

for 296−922 K. This line is also a reasonable fit to the present measurements, except that the smallest k_1 value is 1.8 times larger than the fit. This factor is outside the confidence limits, but the k_1 point at 578 K is the most vulnerable to systematic error because the primary reaction is least well separated from secondary processes. This second k_1 expression is used in the thermochemical analysis below because it covers a wide range of temperature.

Experiments using C_6D_6 instead of benzene at two temperatures are summarized in Table 2 and Figure 5. The results fit

$$k_{1b} = 6.2 \times 10^{-12} \exp(-22.8 \text{ kJ mol}^{-1}/RT) \text{ cm}^3 \text{ molecule}^{-1} \text{ s}^{-1}$$

over 635−922 K.

For the reverse reaction, 28 measurements are summarized in Table 3. No significant dependence is found on the photolysis energy, initial phenyl concentration, and other parameters, which

TABLE 2: Summary of Measurements of the Rate Constant k_{1b} for Cl + C_6D_6

T, K	τ_{res}, s	F, mJ	p, mbar	$[CCl_4]$, 10^{15} molecule cm^{-3}	$[C_6D_6]_{max}$, 10^{15} molecule cm^{-3}	$[Cl]_0$, 10^{12} molecule cm^{-3}	$k_{1b} \pm \sigma_{k1b}$, 10^{-13} cm^3 molecule^{-1} s^{-1}
635	0.9	0.74	71	2.54	2.34 ± 0.08	2.7	2.11 ± 0.14
635	0.9	0.35	71	2.54	2.34 ± 0.08	1.4	1.48 ± 0.17
635	0.9	0.22	69	2.47	1.81 ± 0.06	0.8	1.31 ± 0.07
635	0.9	0.16	69	2.47	1.81 ± 0.06	0.6	1.06 ± 0.06
635[a]							**0.82 ± 0.08**[b]
922	0.4	0.55	42	[c]	0.62 ± 0.02		6.06 ± 0.52
922	0.4	0.26	42	[c]	0.62 ± 0.02		5.52 ± 0.19
923	0.4	0.37	42	[c]	0.68 ± 0.02		6.53 ± 0.92
923	0.4	0.17	42	[c]	0.68 ± 0.02		7.34 ± 0.75
922	0.4	0.75	44	[c]	0.36 ± 0.01		11.75 ± 0.46
922	0.4	0.40	44	[c]	0.36 ± 0.02		4.99 ± 0.53
921	0.3	0.72	41	[c]	0.25 ± 0.02		10.89 ± 1.08
923	0.3	1.03	40	[c]	0.21 ± 0.01		10.22 ± 1.28
923	0.3	0.76	40	[c]	0.21 ± 0.01		8.67 ± 1.09
922[a]							**3.18 ± 0.95**[b]

[a] Average temperature. [b] Extrapolation to zero F. [c] NaCl used as source of Cl rather than CCl_4.

TABLE 3: Summary of Kinetic Measurements in the C_6H_5 + HCl System

T, K	τ_{res}, s	F, mJ	p, mbar	$[C_6H_5I]$, 10^{13} molecule cm^{-3}	$[HCl]_{max}$, 10^{15} molecule cm^{-3}	$[C_6H_5]_0$, 10^{12} molecule cm^{-3}	$k_{-1} \pm \sigma_{k-1}$, 10^{-12} cm^3 molecule^{-1} s^{-1}	$(k_{2'} + k_3) \pm \sigma_{(k2'+k3)}$, s^{-1}	$k_4 \pm \sigma_{k4}$, 10^{-11} cm^3 molecule^{-1} s^{-1}
294	1.2	0.27	50	1.18	1.00 ± 0.03	0.2	9.55 ± 1.15	306 ± 12	2.12 ± 0.07
294	1.2	0.40	51	1.62	0.67 ± 0.02	0.4	9.79 ± 0.77	319 ± 11	2.26 ± 0.07
294	0.6	0.49	25	1.37	0.22 ± 0.01	0.4	9.32 ± 0.69	309 ± 13	2.28 ± 0.14
294[a]							**9.55 ± 0.24**[b]		**2.22 ± 0.09**[b]
330	1.3	0.23	52	2.13	0.88 ± 0.04	0.3	7.53 ± 1.11	327 ± 83	1.19 ± 0.03
331	1.3	0.23	52	2.11	0.70 ± 0.03	0.3	7.87 ± 0.66	412 ± 73	1.19 ± 0.01
330	2.2	0.10	52	3.52	0.98 ± 0.06	0.2	8.67 ± 1.56	543 ± 50	0.71 ± 0.01
330	1.3	0.46	51	2.06	0.84 ± 0.04	0.6	7.82 ± 0.59	368 ± 83	1.22 ± 0.01
330	1.3	0.31	50	2.67	0.40 ± 0.02	0.5	7.51 ± 0.60	397 ± 61	1.11 ± 0.02
330[a]							**7.88 ± 0.47**[b]		**1.08 ± 0.21**[b]
407	1.8	0.36	52	3.00	1.21 ± 0.06	0.7	4.48 ± 0.10	353 ± 31	0.85 ± 0.01
407	1.8	0.17	52	2.98	1.21 ± 0.06	0.3	4.45 ± 0.12	367 ± 14	0.85 ± 0.01
406	1.0	0.29	50	1.64	1.06 ± 0.05	0.3	5.87 ± 0.61	247 ± 31	1.58 ± 0.03
407	1.1	0.34	52	1.70	1.10 ± 0.05	0.4	5.05 ± 1.15	245 ± 26	1.50 ± 0.02
407	1.0	0.22	51	1.65	1.02 ± 0.05	0.2	5.51 ± 0.35	222 ± 20	1.61 ± 0.05
407	1.0	0.18	51	1.67	0.75 ± 0.03	0.2	5.41 ± 0.39	242 ± 33	1.59 ± 0.03
407[a]							**5.13 ± 0.58**[b]		**1.33 ± 0.37**[b]
545	1.0	0.85	51	0.63	0.55 ± 0.02	0.3	3.08 ± 0.35	106 ± 8	3.86 ± 1.49
545	1.0	0.62	51	0.63	0.55 ± 0.02	0.2	3.14 ± 0.41	104 ± 8	3.30 ± 3.21
542	0.6	0.72	51	0.34	0.47 ± 0.02	0.2	3.88 ± 0.28	97 ± 5	6.72 ± 3.38
545	1.0	0.65	51	1.13	0.41 ± 0.02	0.5	4.31 ± 0.76	62 ± 3	2.59 ± 1.92
544	1.0	0.37	49	0.61	0.53 ± 0.02	0.1	2.78 ± 0.25	172 ± 120	5.89 ± 0.73
544[a]							**3.44 ± 0.63**[b]		**4.47 ± 1.76**[b]
749	1.0	0.84	52	2.15	0.55 ± 0.03	1.1	3.43 ± 0.34	305 ± 56	1.25 ± 0.11
749	0.6	0.47	54	1.26	0.48 ± 0.02	0.4	3.32 ± 0.32	208 ± 55	2.00 ± 0.35
745	0.5	0.24	25	1.06	0.54 ± 0.03	0.2	1.87 ± 0.64	226 ± 64	2.79 ± 0.34
746	0.5	0.79	26	1.10	0.52 ± 0.02	0.6	4.12 ± 0.35	163 ± 31	2.95 ± 0.46
747	0.5	0.46	27	1.14	0.53 ± 0.03	0.3	3.10 ± 0.29	162 ± 41	2.26 ± 0.54
746	1.0	0.41	54	1.73	0.66 ± 0.03	0.4	1.80 ± 0.21	170 ± 42	1.81 ± 0.77
750	1.1	0.25	53	2.21	0.68 ± 0.02	0.3	2.73 ± 0.21	213 ± 56	2.13 ± 0.22
750	1.0	0.31	52	2.09	0.65 ± 0.02	0.4	2.23 ± 0.19	272 ± 47	2.03 ± 0.19
750	1.0	0.35	52	2.09	0.65 ± 0.02	0.5	3.14 ± 0.27	233 ± 38	2.27 ± 0.34
748[a]							**2.86 ± 0.77**[b]		**2.17 ± 0.50**[b]

[a] Average temperature. [b] Average rate constant.

indicates k_{-1} has been isolated from secondary processes. The mean values at each temperature are plotted in Arrhenius form on Figure 6 and yield

$$k_{-1} = (1.14 \pm 0.13) \times 10^{-12} \exp(+5.2 \pm 0.3 \text{ kJ mol}^{-1}/RT) \text{ cm}^3 \text{ molecule}^{-1} \text{ s}^{-1}$$

over 294−748 K. The 2σ statistical uncertainties in the fitted k_{-1} lie between 6 and 12%, and we propose overall confidence limits of ±13%.

Eight measurements with the deuterated analog −1c at two temperatures are listed in Table 4, and the data may be summarized as

$$k_{-1c} = 7.7 \times 10^{-13} \exp(+4.9 \text{ kJ mol}^{-1}/RT) \text{ cm}^3 \text{ molecule}^{-1} \text{ s}^{-1}$$

over 292−546 K.

These studies also yield information about eqs 2 and 4, which is summarized in Tables 3 and 4. As noted above, an upper limit to k_2 was estimated by dividing the B term by $[C_6H_5I]$.

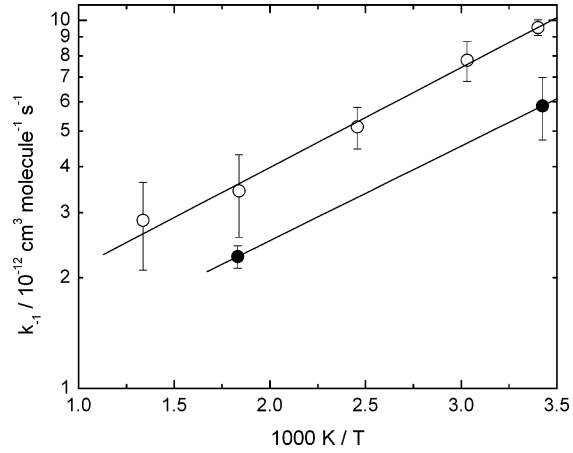

Figure 6. Arrhenius plot of k_{-1} and k_{-1c}. Open circles: HCl + C_6H_5; filled circles: DCl + C_6H_5. Error bars represent $\pm 1\sigma$.

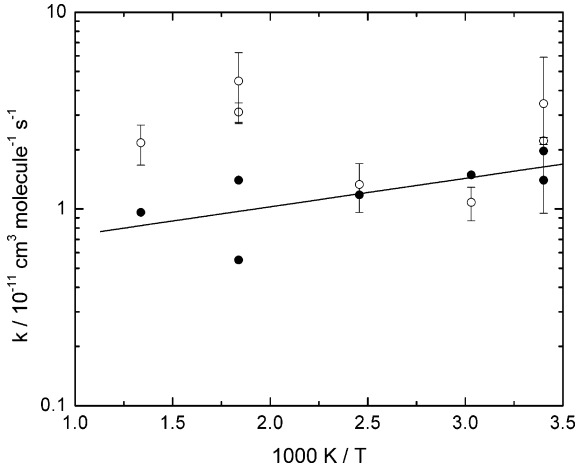

Figure 7. Arrhenius plot of k_2 for the Cl + C_6H_5I reaction, solid circles (upper limit) and line, and k_4 for the C_6H_5 + C_6H_5I reaction, open circles with 1σ error bars.

The lowest values obtained at each temperature, in experiments with both HCl and DCl, are plotted in Arrhenius form on Figure 7 and can be approximately expressed as

$$k_2 \leq 5.3 \times 10^{-12} \exp(+2.8 \text{ kJ mol}^{-1}/RT) \text{ cm}^3 \text{ molecule}^{-1} \text{ s}^{-1}$$

over 300−750 K. Given the scatter, an uncertainty of at least a factor of 1.5 in k_2 is suggested. Figure 7 also shows the k_4 values from both sets of experiments, which exhibit considerable scatter. These data may be summarized approximately as $k_4 = (2 \pm 1) \times 10^{-11}$ cm^3 molecule^{-1} s^{-1} over 300−750 K.

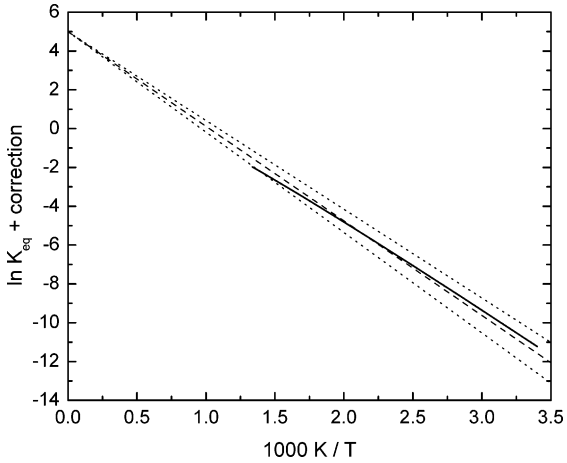

Figure 8. van't Hoff plot for the equilibrium constant of Cl + C_6H_6 = HCl + C_6H_5 (solid line, experiment; dashed line, third-law fit with $\Delta_r H_{298} = 40.5$ kJ mol^{-1} constrained to pass through computed $\Delta S_{298}/R$). Dotted lines indicate $\Delta_r H_{298} = 38.0$ and 43.0 kJ mol^{-1}.

3.2. Thermochemistry. The ratio k_1/k_{-1} equals the equilibrium constant $K_{eq} = 53.5 \exp(-4430\ K/T)$ in the overlapping temperature range 296−748 K. We evaluated K_{eq} at 10 temperatures from this expression and used a van't Hoff plot (Figure 8) to derive $\Delta_r H_{298}$ for eq 1 via a third-law method. This plot includes a temperature correction[13] of $-(\Delta S_T - \Delta S_{298})/R + (\Delta H_T - \Delta H_{298})/RT$ to ln K_{eq}. The correction is ≤ 0.14. The temperature dependences of ΔS and ΔH were evaluated via ΔC_p for eq 1, which was derived as follows. Thermochemical data for Cl and HCl were taken from the JANAF tables,[26] while data for C_6H_6 and C_6H_5 were calculated via standard relations[26] from moments of inertia and vibrational frequencies and are listed in Table 1S of the Supporting Information. Frequencies for C_6H_6 were taken from Shimanouchi's tabulation[27] and frequencies for C_6H_5 were taken from the work of Łapiński et al.[28] We computed the product of the moments of inertia for C_6H_5 to be 5.61×10^{-135} kg^3 m^6 using QCISD/6-31G(d) theory, which was chosen because it reproduced the known value for C_6H_6 to within 0.2%. The linear fit to the van't Hoff plot was constrained to have an intercept equal to our derived $\Delta S_{298} = 41.50$ J K^{-1} mol^{-1} divided by R. The slope of this line is $-\Delta H_{298}/R$, from which we obtain $\Delta H_{298} = 40.5$ kJ mol^{-1}. The maximum deviation from the fit in Figure 8 is 0.5. The uncertainty in ΔH_{298} is estimated via an assumed factor of 2 uncertainty in the central K_{eq} value, arising mainly from uncertainty in k_1. This leads to confidence limits for ΔH_{298} of ± 2.5 kJ mol^{-1}, and this is shown graphically in Figure 8. Addition of the bond dissociation enthalpy D_{298}(H−Cl)[26] yields $D_{298}(C_6H_5\text{−H}) = 472.1 \pm 2.5$ kJ mol^{-1}. Combination of this quantity with the enthalpies of formation $\Delta_f H_{298}(C_6H_6)$[29] = 82.9

TABLE 4: Summary of Kinetic Measurements in the C_6H_5 + DCl System

T, K	τ_{res}, s	F, mJ	p, mbar	$[C_6H_5I]$, 10^{13} molecule cm^{-3}	$[DCl]_{max}$, 10^{15} molecule cm^{-3}	$[C_6H_5]_0$, 10^{12} molecule cm^{-3}	$k_{-1b} \pm \sigma_{k-1b}$, 10^{-12} cm^3 molecule^{-1} s^{-1}	$(k_{2b'} + k_{3b}) \pm \sigma_{(k2b'+k3b)}$, s^{-1}	$k_{4b} \pm \sigma_{k4b}$, 10^{-11} cm^3 molecule^{-1} s^{-1}
292	0.7	0.64	25	2.44	0.35 ± 0.01	1.0	4.93 ± 1.73	345 ± 52	2.16 ± 0.02
292	0.7	0.36	25	2.44	0.35 ± 0.01	0.6	5.61 ± 1.58	329 ± 104	4.17 ± 0.03
292	0.9	0.45	25	2.50	0.26 ± 0.01	0.7	7.72 ± 0.76	432 ± 43	7.41 ± 0.04
292	0.9	0.32	25	2.51	0.26 ± 0.01	0.5	5.99 ± 1.12	441 ± 42	2.22 ± 0.01
292	0.7	0.59	25	2.38	0.40 ± 0.01	0.9	5.00 ± 0.75	513 ± 74	1.17 ± 0.01
292[a]							5.85 ± 1.13[b]		**3.43 ± 2.48**[b]
546	0.5	0.89	25	1.38	0.20 ± 0.01	0.8	2.19 ± 0.34	190 ± 18	2.82 ± 0.27
546	0.5	0.39	25	1.38	0.20 ± 0.01	0.3	2.46 ± 0.22	191 ± 15	3.01 ± 0.36
546	0.4	0.48	25	1.41	0.23 ± 0.01	0.4	2.19 ± 0.44	206 ± 9	3.50 ± 0.21
546[a]							2.28 ± 0.16[b]		**3.11 ± 0.35**[b]

[a] Average temperature. [b] Average rate constant.

$\pm$ 0.5 and $\Delta_f H_{298}(H)$[26] = 218.0 kJ mol^{-1} yields $\Delta_f H_{298}(C_6H_5)$ = 337.0 $\pm$ 2.5 kJ mol^{-1}.

4. Discussion

There are no prior k_{-1} measurements for comparison. The analogous C_6H_5 + HBr reaction has been investigated by Yu and Lin,[30] who found a similar order of magnitude for the rate constant with E_a = 4.6 $\pm$ 1.7 kJ mol^{-1}, which by contrast to E_a for eq -1 is a positive value. Our results might be rationalized in terms of a potential surface qualitatively similar to that discussed for CH_3 + HBr,[31] which involved formation of a bound intermediate followed by dissociation to final products over a barrier below the initial reactants. Computational studies are under way to test this idea. Adduct formation between Cl and C_6H_6 has been discussed, but the binding energy in the chlorocyclohexadienyl adduct[6] of 30 $\pm$ 10 kJ mol^{-1} is too small for the adduct to be significant at elevated temperatures. The kinetic isotope effect $k_H/k_D > 1$ for both k_{-1} and k_1 is consistent with a mechanism where C$-$H bond breaking is rate-limiting.

The room-temperature values of k_1 determined by Shi and Bernhard[5] and Sokolov et al.[6] divided by our k_{-1} yield K_{eq} and thus ΔG, which together with our calculated ΔS yields ΔH. Their results imply $D_{298}(C_6H_5{-}H)$ = 466 $\pm$ 1 and 472 $\pm$ 3 kJ mol^{-1}, respectively. For comparison, a recent assessment is 474.9 $\pm$ 2.5 kJ mol^{-1}.[7] Therefore, the Shi and Bernhard rate constant appears somewhat too high, and we employed the Sokolov et al. value in our recommendation for k_1 above. This k_1 and our k_{-1} yield $\Delta_f H_{298}(C_6H_5)$ kJ mol^{-1} = 337.0 $\pm$ 2.5 kJ mol^{-1}, a result which is in agreement with the recent determinations of 339.4 $\pm$ 2.5 and 338 $\pm$ 3 kJ mol^{-1}.[7,8] Thus, we support a revision upward from prior recommendations, for example, those of 328.9 $\pm$ 8.4 kJ mol^{-1} by McMillen and Golden[32] and 330.1 $\pm$ 3.3 kJ mol^{-1} by Berkowitz et al.[33] Our value agrees with an early kinetic value of 334.7 $\pm$ 4.2 kJ mol^{-1} obtained by Rodgers et al.,[34] who combined their measured activation energy for $C_6H_5I + I \rightarrow C_6H_5 + I_2$ with an assumed 0 $\pm$ 4.2 kJ mol^{-1} activation energy for the reverse reaction. This assumption appears to be valid.

Our k_2 expression yields an upper limit of 1.7 $\times$ 10^{-11} cm^3 molecule^{-1} s^{-1} at 296 K, with an uncertainty of a factor of 1.5. Because diffusion of atomic Cl is likely modest compared to this reaction, k_2 may be close to this limit. There is reasonable accord with the smog chamber measurement of (3.3 $\pm$ 0.7) $\times$ 10^{-11} cm^3 molecule^{-1} s^{-1}.[16] Andersen et al. speculated that the mechanism for eq 2 involves addition of Cl to C_6H_5I followed by elimination of I. The small negative E_a proposed here is consistent with a barrierless addition step. There are no prior data with which to compare our approximate estimate for k_4 for the phenyl + phenyl iodide reaction. The magnitude suggests little or no energy barrier, and plausible products by analogy with eq 2 are biphenyl + I atoms.

5. Conclusions

The reaction of phenyl with HCl has been studied for the first time, and a negative E_a is found. A recommended rate constant for Cl + benzene is derived from our high-temperature measurements and literature data at room temperature. The kinetic isotope effects in both directions support an abstraction mechanism. Third-law analysis of the equilibrium constant yields thermochemistry in accord with other recent determinations of the enthalpy of formation of C_6H_5. Our k_1 and k_{-1} measurements, the room-temperature result for k_1 by Sokolov et al.,[6] and recommended thermochemistry for C_6H_5[7,8] together form a consistent picture.

Acknowledgment. We thank Kimberly Destefani, Dennis Hu, Jade Kumar, Prashan Shanthakumar, and Chester Wu for assistance with some of the experiments. This work was supported by the Robert A. Welch Foundation (Grant B-1174) and the UNT Faculty Research Fund. We are also grateful for support from the NSF REU program (JPS) through grant CHE-0243795 and from the Texas Academy of Mathematics and Science (AM).

Supporting Information Available: Thermodynamic functions for benzene and phenyl as a function of temperature. This material is available free of charge via the Internet at http://pubs.acs.org.

References and Notes

(1) Miller, J. A.; Pilling, M. J.; Troe, J. *Proc. Combust. Inst.* **2005**, *30*, 43.
(2) Atkinson, R.; Aschmann, S. M. *Int. J. Chem. Kinet.* **1985**, *17*, 33.
(3) Wallington, T. J.; Skewes, L. M.; Siegl, W. O. *J. Photochem. Photobiol., A* **1988**, *45*, 167.
(4) Nozière, B.; Lesclaux, R.; Veyret, B. *J. Phys. Chem.* **1990**, *98*, 2864.
(5) Shi, J.; Bernhard, M. *Int. J. Chem. Kinet.* **1997**, *29*, 349.
(6) Sokolov, O.; Hurley, M. D.; Wallington, T. J.; Kaiser, E. W.; Platz, J.; Nielsen, O. J.; Berho, F.; Rayez, M.-T.; Lesclaux, R. *J. Phys. Chem. A* **1998**, *102*, 10671.
(7) Davico, G. E.; Bierbaum, V. M.; DePuy, C. H.; Ellison, G. B.; Squires, R. R. *J. Am. Chem. Soc.* **1995**, *117*, 2590.
(8) Heckmann, E.; Hippler, H.; Troe, J. *Proc. Combust. Inst.* **1996**, *26*, 543.
(9) Russell, J. J.; Seetula, J. A.; Gutman, D. *J. Am. Chem. Soc.* **1988**, *110*, 3092.
(10) Seakins, P. W.; Pilling, M. J.; Niiranen, J. T.; Gutman, D.; Krasnoperov, L. N. *J. Phys. Chem.* **1992**, *96*, 9847.
(11) Nicovich, J. M.; Van Dijk, C. A.; Kreutter, K. D.; Wine, P. H. *J. Phys. Chem.* **1991**, *95*, 9890.
(12) Niiranen, J. T.; Gutman, D.; Krasnoperov, L. N. *J. Phys. Chem.* **1992**, *96*, 5881.
(13) Kalinovski, I. J.; Gutman, D.; Krasnoperov, L. N.; Goumri, A.; Yuan, W.-J.; Marshall, P. *J. Phys. Chem.* **1994**, *98*, 9551.
(14) Seetula, J. A. *Phys. Chem. Chem. Phys.* **2002**, *4*, 455.
(15) Benson, S. W.; Dobis, O. *J. Phys. Chem. A* **1998**, *102*, 5175.
(16) Andersen, M. P. S.; Ponomarev, D. A.; Nielsen, O. J.; Hurley, M. D.; Wallington, T. J. *Chem. Phys. Lett.* **2001**, *350*, 423.
(17) Shi, Y.; Marshall, P. *J. Phys. Chem.* **1991**, *95*, 1654.
(18) Ding, L.; Marshall, P. *J. Phys. Chem.* **1992**, *96*, 2197.
(19) Hanf, A.; Läuter, A.; Volpp, H.-R. *Chem. Phys. Lett.* **2003**, *368*, 445.
(20) Adusei, G. Y.; Fontijn, A. *Proc. Combust. Inst.* **1994**, *25*, 801.
(21) Marshall, P. *Comput. Chem.* **1987**, *11*, 219.
(22) Marshall, P. *Comput. Chem.* **1989**, *13*, 103.
(23) Irvin, J. A.; Quickenden, T. I. *J. Chem. Educ.* **1983**, *60*, 711.
(24) Pence, W. H.; Baughcum, S. L.; Leone, S. R. *J. Phys. Chem.* **1981**, *85*, 3844.
(25) Adusei, G. Y.; Fontijn, A. *J. Phys. Chem.* **1993**, *97*, 1409.
(26) *NIST-JANAF Thermochemical Tables*, 4th ed.; Chase, M. W., Jr., Ed.; American Chemical Society and the American Institute of Physics: Woodbury, New York, 1998.
(27) Shimanouchi, T. *Tables of Molecular Vibrational Frequencies*; National Bureau of Standards: Gaithersburg, Maryland, 1972; Consolidated Volume I.
(28) Łapiński, A.; Spanget-Larsen, J.; Langgård, M.; Waluk, J.; Radziszewski, J. G. *J. Phys. Chem. A* **2001**, *105*, 10520.
(29) Prosen, E. J.; Johnson, W. H.; Rossini, F. D. *J. Res. Natl. Bur. Stand.* **1946**, *36*, 455.
(30) Yu, T.; Lin, M. C. *Int. J. Chem. Kinet.* **1994**, *26*, 771.
(31) Krasnoperov, L. N.; Peng, J.; Marshall, P. *J. Phys. Chem. A* **2006**, *110*, 3110.
(32) McMillen, D. F.; Golden, D. M. *Ann. Rev. Phys. Chem.* **1982**, *33*, 493.
(33) Berkowitz, J.; Ellison, G. B.; Gutman, D. *J. Phys. Chem.* **1994**, *98*, 2744.
(34) Rodgers, A. S.; Golden, D. M.; Benson, S. W. *J. Am. Chem. Soc.* **1967**, *89*, 4578.